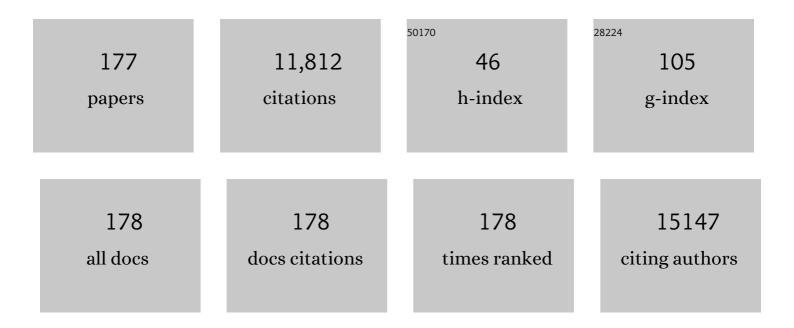
List of Publications by Year in descending order

Source: https://exaly.com/author-pdf/11381240/publications.pdf Version: 2024-02-01



#	Article	IF	CITATIONS
1	Highly stretchable and tough hydrogels. Nature, 2012, 489, 133-136.	13.7	4,089
2	Highly stretchable, transparent ionic touch panel. Science, 2016, 353, 682-687.	6.0	818
3	Microscale spherical carbon-coated Li4Ti5O12 as ultra high power anode material for lithium batteries. Energy and Environmental Science, 2011, 4, 1345.	15.6	433
4	Double Carbon Coating of LiFePO <sub>4</sub> as High Rate Electrode for Rechargeable Lithium Batteries. Advanced Materials, 2010, 22, 4842-4845.	11.1	361
5	Stable silicon-ionic liquid interface for next-generation lithium-ion batteries. Nature Communications, 2015, 6, 6230.	5.8	212
6	Wrinkled hard skins on polymers created by focused ion beam. Proceedings of the National Academy of Sciences of the United States of America, 2007, 104, 1130-1133.	3.3	203
7	Electric current-induced annealing during uniaxial tension of aluminum alloy. Scripta Materialia, 2014, 75, 58-61.	2.6	186
8	Nanoscale Interface Modification of LiCoO <sub>2</sub> by Al <sub>2</sub> O <sub>3</sub> Atomic Layer Deposition for Solid-State Li Batteries. Journal of the Electrochemical Society, 2012, 159, A1120-A1124.	1.3	173
9	Reversible Highâ€Capacity Si Nanocomposite Anodes for Lithiumâ€ion Batteries Enabled by Molecular Layer Deposition. Advanced Materials, 2014, 26, 1596-1601.	11.1	169
10	Solid State Enabled Reversible Four Electron Storage. Advanced Energy Materials, 2013, 3, 120-127.	10.2	155
11	A new criterion for internal crack formation in continuously cast steels. Metallurgical and Materials Transactions B: Process Metallurgy and Materials Processing Science, 2000, 31, 779-794.	1.0	154
12	Folding wrinkles of a thin stiff layer on aÂsoft substrate. Proceedings of the Royal Society A: Mathematical, Physical and Engineering Sciences, 2012, 468, 932-953.	1.0	142
13	Conformal Coatings of Cyclizedâ€₽AN for Mechanically Resilient Si nano omposite Anodes. Advanced Energy Materials, 2013, 3, 697-702.	10.2	134
14	lonic Liquid Enabled FeS <sub>2</sub> for Highâ€Energyâ€Đensity Lithiumâ€Ion Batteries. Advanced Materials, 2014, 26, 7386-7392.	11.1	116
15	Liquid Metal Nanoparticles as Initiators for Radical Polymerization of Vinyl Monomers. ACS Macro Letters, 2019, 8, 1522-1527.	2.3	109
16	Electric current–assisted deformation behavior of Al-Mg-Si alloy under uniaxial tension. International Journal of Plasticity, 2017, 94, 148-170.	4.1	106
17	Structure and mechanical properties of Ag-incorporated DLC films prepared by a hybrid ion beam deposition system. Thin Solid Films, 2007, 516, 248-251.	0.8	103
18	A Stabilized PANâ€FeS <sub>2</sub> Cathode with an EC/DEC Liquid Electrolyte. Advanced Energy Materials, 2014, 4, 1300961.	10.2	100

#	Article	IF	CITATIONS
19	A Highly Reversible Nano‣i Anode Enabled by Mechanical Confinement in an Electrochemically Activated Li <sub>x</sub> Ti <sub>4</sub> Ni <sub>4</sub> Si <sub>7</sub> Matrix. Advanced Energy Materials, 2012, 2, 1226-1231.	10.2	94
20	Effect of -Carbon and Sulfur in Continuously Cast Strand on Longitudinal Surface Cracks ISIJ International, 1996, 36, 284-289.	0.6	92
21	Effect of Pores in Hollow Carbon Nanofibers on Their Negative Electrode Properties for a Lithium Rechargeable Battery. ACS Applied Materials & Interfaces, 2012, 4, 6702-6710.	4.0	84
22	Highly Stretchable and Notch-Insensitive Hydrogel Based on Polyacrylamide and Milk Protein. ACS Applied Materials & Interfaces, 2016, 8, 29220-29226.	4.0	81
23	Experimental Realization of Few Layer Two-Dimensional MoS <sub>2</sub> Membranes of Near Atomic Thickness for High Efficiency Water Desalination. Nano Letters, 2019, 19, 5194-5204.	4.5	80
24	Horizontal-to-Vertical Transition of 2D Layer Orientation in Low-Temperature Chemical Vapor Deposition-Grown PtSe <sub>2</sub> and Its Influences on Electrical Properties and Device Applications. ACS Applied Materials & Interfaces, 2019, 11, 13598-13607.	4.0	77
25	Co-precipitation synthesis of micro-sized spherical LiMn0.5Fe0.5PO4 cathode material for lithium batteries. Journal of Materials Chemistry, 2011, 21, 19368.	6.7	75
26	Unexpected high power performance of atomic layer deposition coated Li[Ni1/3Mn1/3Co1/3]O2 cathodes. Journal of Power Sources, 2014, 254, 190-197.	4.0	73
27	Interface-enhanced Li ion conduction in a LiBH <sub>4</sub> –SiO <sub>2</sub> solid electrolyte. Physical Chemistry Chemical Physics, 2016, 18, 22540-22547.	1.3	72
28	Effect of Cooling Rate on ZST, LIT and ZDT of Carbon Steels Near Melting Point ISIJ International, 1998, 38, 1093-1099.	0.6	71
29	Direct Growth of Compound Semiconductor Nanowires by On-Film Formation of Nanowires: Bismuth Telluride. Nano Letters, 2009, 9, 2867-2872.	4.5	67
30	Prediction of cracks in continuously cast steel beam blank through fully coupled analysis of fluid flow, heat transfer, and deformation behavior of a solidifying shell. Metallurgical and Materials Transactions A: Physical Metallurgy and Materials Science, 2000, 31, 225-237.	1.1	61
31	Microstructure Study of Electrochemically Driven Li <sub>x</sub> Si. Advanced Energy Materials, 2011, 1, 1199-1204.	10.2	61
32	Extreme wettability of nanostructured glass fabricated by non-lithographic, anisotropic etching. Scientific Reports, 2015, 5, 9362.	1.6	60
33	Multifunctional Two-Dimensional PtSe <sub>2</sub> -Layer Kirigami Conductors with 2000% Stretchability and Metallic-to-Semiconducting Tunability. Nano Letters, 2019, 19, 7598-7607.	4.5	59
34	Phase Analysis of Steels by Grain-averaged EBSD Functions. ISIJ International, 2011, 51, 130-136.	0.6	58
35	UV-responsive nano-sponge for oil absorption and desorption. Scientific Reports, 2015, 5, 12908.	1.6	57
36	Measurements of stress and fracture in germanium electrodes of lithium-ion batteries during electrochemical lithiation and delithiation. Journal of Power Sources, 2016, 304, 164-169.	4.0	57

#	Article	IF	CITATIONS
37	Enhanced Li Ion Conductivity in LiBH <sub>4</sub> –Al <sub>2</sub> O <sub>3</sub> Mixture via Interface Engineering. Journal of Physical Chemistry C, 2017, 121, 26209-26215.	1.5	57
38	A Finite Element Model for 2-Dimensional Slice of Cast Strand ISIJ International, 1999, 39, 445-454.	0.6	52
39	Mechanical Behavior of Carbon Steels in the Temperature Range of Mushy Zone ISIJ International, 2000, 40, 356-363.	0.6	52
40	Controlled formation of nanoscale wrinkling patterns on polymers using focused ion beam. Scripta Materialia, 2007, 57, 747-750.	2.6	51
41	Thickness-Independent Semiconducting-to-Metallic Conversion in Wafer-Scale Two-Dimensional PtSe <sub>2</sub> Layers by Plasma-Driven Chalcogen Defect Engineering. ACS Applied Materials & Interfaces, 2020, 12, 14341-14351.	4.0	51
42	FeS <sub>2</sub> â€Imbedded Mixed Conducting Matrix as a Solid Battery Cathode. Advanced Energy Materials, 2016, 6, 1600495.	10.2	50
43	An All-Solid-State Li-Ion Battery with a Pre-Lithiated Si-Ti-Ni Alloy Anode. Journal of the Electrochemical Society, 2013, 160, A1497-A1501.	1.3	49
44	Tensile deformation behavior of stainless steel clad aluminum bilayer sheet. Materials Science & Engineering A: Structural Materials: Properties, Microstructure and Processing, 1997, 222, 158-165.	2.6	48
45	Bioinspired steel surfaces with extreme wettability contrast. Nanoscale, 2012, 4, 2900.	2.8	48
46	Wafer-Scale Growth of 2D PtTe <sub>2</sub> with Layer Orientation Tunable High Electrical Conductivity and Superior Hydrophobicity. ACS Applied Materials & Interfaces, 2020, 12, 10839-10851.	4.0	48
47	Hierarchical Porous Framework of Siâ€Based Electrodes for Minimal Volumetric Expansion. Advanced Materials, 2014, 26, 3520-3525.	11.1	47
48	Microstructural evolution of NbF5-doped MgH2 exhibiting fast hydrogen sorption kinetics. Journal of Power Sources, 2008, 178, 373-378.	4.0	46
49	Water condensation behavior on the surface of a network of superhydrophobic carbon fibers with high-aspect-ratio nanostructures. Carbon, 2012, 50, 5085-5092.	5.4	46
50	Controlled epitaxial growth modes of ZnO nanostructures using different substrate crystal planes. Journal of Materials Chemistry, 2009, 19, 941.	6.7	45
51	Adhesion behavior of mouse liver cancer cells on nanostructured superhydrophobic and superhydrophilic surfaces. Soft Matter, 2013, 9, 8705.	1.2	45
52	Thermal stability of superhydrophobic, nanostructured surfaces. Journal of Colloid and Interface Science, 2013, 391, 152-157.	5.0	45
53	Centimeter-scale Green Integration of Layer-by-Layer 2D TMD vdW Heterostructures on Arbitrary Substrates by Water-Assisted Layer Transfer. Scientific Reports, 2019, 9, 1641.	1.6	44
54	Two-Dimensional Near-Atom-Thickness Materials for Emerging Neuromorphic Devices and Applications. IScience, 2020, 23, 101676.	1.9	44

#	Article	IF	CITATIONS
55	Texture and Deformation Behaviour through Thickness Direction in Strip-cast 4.5wt% Si Steel Sheet ISIJ International, 2000, 40, 1210-1215.	0.6	43
56	Orientation rotation behavior during in situ tensile deformation of polycrystalline 1050 aluminum alloy. International Journal of Mechanical Sciences, 2003, 45, 1613-1623.	3.6	43
57	Plasmaâ€Induced Heteroâ€Nanostructures on a Polymer with Selective Metal Coâ€Deposition. Advanced Materials Interfaces, 2015, 2, 1400431.	1.9	41
58	Analysis of hot forging of porous metals. Materials Science & Engineering A: Structural Materials: Properties, Microstructure and Processing, 1996, 206, 81-89.	2.6	40
59	Fracture behavior of diamond-like carbon films on stainless steel under a micro-tensile test condition. Diamond and Related Materials, 2006, 15, 38-43.	1.8	40
60	Precipitation of austenite particles at grain boundaries during aging of Fe-Mn-Ni steel. Metallurgical and Materials Transactions A: Physical Metallurgy and Materials Science, 2002, 33, 1057-1067.	1.1	38
61	Microstructural evolution induced by micro-cracking during fast lithiation of single-crystalline silicon. Journal of Power Sources, 2014, 265, 160-165.	4.0	38
62	Unraveling the Origin and Mechanism of Nanofilament Formation in Polycrystalline SrTiO <sub>3</sub> Resistive Switching Memories. Advanced Materials, 2019, 31, e1901322.	11.1	38
63	A three-dimensional model of the spray forming method. Metallurgical and Materials Transactions B: Process Metallurgy and Materials Processing Science, 1998, 29, 699-708.	1.0	37
64	Facile conductive bridges formed between silicon nanoparticles inside hollow carbon nanofibers. Nanoscale, 2013, 5, 4790.	2.8	37
65	Optimized Silicon Electrode Architecture, Interface, and Microgeometry for Nextâ€Generation Lithiumâ€ion Batteries. Advanced Materials, 2016, 28, 188-193.	11.1	37
66	Model for compaction of metal powders. International Journal of Mechanical Sciences, 1999, 41, 121-141.	3.6	36
67	A Fully Coupled Analysis of Fluid Flow, Heat Transfer and Stress in Continuous Round Billet Casting ISIJ International, 1999, 39, 435-444.	0.6	36
68	Simple and inexpensive coal-tar-pitch derived Si-C anode composite for all-solid-state Li-ion batteries. Solid State Ionics, 2018, 324, 207-217.	1.3	36
69	Strainâ€Driven and Layerâ€Numberâ€Dependent Crossover of Growth Mode in van der Waals Heterostructures: 2D/2D Layerâ€By‣ayer Horizontal Epitaxy to 2D/3D Vertical Reorientation. Advanced Materials Interfaces, 2018, 5, 1800382.	1.9	35
70	Vertically Aligned 2D MoS <sub>2</sub> Layers with Strain-Engineered Serpentine Patterns for High-Performance Stretchable Gas Sensors: Experimental and Theoretical Demonstration. ACS Applied Materials & Interfaces, 2020, 12, 53174-53183.	4.0	35
71	Wetting behaviours of a-C:H:Si:O film coated nano-scale dual rough surface. Chemical Physics Letters, 2007, 436, 199-203.	1.2	33
72	Metallophobic Coatings to Enable Shape Reconfigurable Liquid Metal Inside 3D Printed Plastics. ACS Applied Materials & Interfaces, 2021, 13, 12709-12718.	4.0	33

#	Article	IF	CITATIONS
73	Tin Networked Electrode Providing Enhanced Volumetric Capacity and Pressureless Operation for All-Solid-State Li-Ion Batteries. Journal of the Electrochemical Society, 2015, 162, A711-A715.	1.3	32
74	A simple technique for measuring the fracture energy of lithiated thin-film silicon electrodes at various lithium concentrations. Journal of Power Sources, 2015, 294, 159-166.	4.0	32
75	Wafer-Scale Two-Dimensional MoS <sub>2</sub> Layers Integrated on Cellulose Substrates Toward Environmentally Friendly Transient Electronic Devices. ACS Applied Materials & Interfaces, 2020, 12, 25200-25210.	4.0	31
76	Hierarchical structures of AlOOH nanoflakes nested on Si nanopillars with anti-reflectance and superhydrophobicity. Nanoscale, 2013, 5, 10014.	2.8	30
77	Effects of surface nanostructures on self-cleaning and anti-fogging characteristics of transparent glass. Journal of Mechanical Science and Technology, 2017, 31, 5407-5414.	0.7	30
78	High Temperature Deformation Behavior of Carbon Steel in the Austenite and .DELTAFerrite Regions ISIJ International, 1999, 39, 91-98.	0.6	29
79	Microstructural change of 2LiBH4/Al with hydrogen sorption cycling: Separation of Al and B. Scripta Materialia, 2009, 60, 1089-1092.	2.6	28
80	Centimeter-Scale 2D van der Waals Vertical Heterostructures Integrated on Deformable Substrates Enabled by Gold Sacrificial Layer-Assisted Growth. Nano Letters, 2017, 17, 6157-6165.	4.5	28
81	In Situ Engineering of the Electrode–Electrolyte Interface for Stabilized Overlithiated Cathodes. Advanced Materials, 2017, 29, 1604549.	11.1	26
82	Analysis of the deformation of a perforated sheet under uniaxial tension. Journal of Materials Processing Technology, 1996, 58, 139-144.	3.1	25
83	Reduction of the residual compressive stress of tetrahedral amorphous carbon film by Ar background gas during the filtered vacuum arc process. Journal of Applied Physics, 2007, 101, 023504.	1.1	25
84	High Performance Gas Diffusion Layer with Hydrophobic Nanolayer under a Supersaturated Operation Condition for Fuel Cells. ACS Applied Materials & Interfaces, 2015, 7, 5506-5513.	4.0	25
85	Automated Assembly of Wafer-Scale 2D TMD Heterostructures of Arbitrary Layer Orientation and Stacking Sequence Using Water Dissoluble Salt Substrates. Nano Letters, 2020, 20, 3925-3934.	4.5	25
86	Towards the Commercialization of the All-Solid-State Li-ion Battery: Local Bonding Structure and the Reversibility of Sheet-Style Si-PAN Anodes. Journal of the Electrochemical Society, 2020, 167, 060522.	1.3	25
87	In situ transmission electron microscopy study on microstructural changes in NbF5-doped MgH2 during dehydrogenation. Scripta Materialia, 2010, 62, 701-704.	2.6	24
88	Face-Centered-Cubic Lithium Crystals Formed in Mesopores of Carbon Nanofiber Electrodes. ACS Nano, 2013, 7, 5801-5807.	7.3	24
89	Gelation dynamics of ionically crosslinked alginate gel with various cations. Macromolecular Research, 2015, 23, 1112-1116.	1.0	24
90	Microtexture development during equibiaxial tensile deformation in monolithic and dual phase steels. Acta Materialia, 2011, 59, 5462-5471.	3.8	23

#	Article	IF	CITATIONS
91	Pd effect on reliability of Ag bonding wires in microelectronic devices in high-humidity environments. Metals and Materials International, 2012, 18, 881-885.	1.8	22
92	Wafer-scale 2D PtTe <sub>2</sub> layers for high-efficiency mechanically flexible electro-thermal smart window applications. Nanoscale, 2020, 12, 10647-10655.	2.8	22
93	Large-area 2D TMD layers for mechanically reconfigurable electronic devices. Journal Physics D: Applied Physics, 2020, 53, 313002.	1.3	22
94	Electrochemically induced and orientation dependent crack propagation in single crystal silicon. Journal of Power Sources, 2014, 267, 739-743.	4.0	21
95	Wafer-scale 2D PtTe2 layers-enabled Kirigami heaters with superior mechanical stretchability and electro-thermal responsiveness. Applied Materials Today, 2020, 20, 100718.	2.3	21
96	Nanoscale ripples on polymers created by a focused ion beam. Nanotechnology, 2009, 20, 115301.	1.3	20
97	Nitriding of Interstitial Free Steel in Potassium–Nitrate Salt Bath. ISIJ International, 2006, 46, 111-120.	0.6	19
98	Nanostructures formed on carbon-based materials with different levels of crystallinity using oxygen plasma treatment. Thin Solid Films, 2015, 590, 324-329.	0.8	19
99	Nanostructured Si/C Fibers as a Highly Reversible Anode Material for All-Solid-State Lithium-Ion Batteries. Journal of the Electrochemical Society, 2018, 165, A1903-A1908.	1.3	19
100	Investigation of the material flow and texture evolution in friction-stir welded aluminum alloy. Metals and Materials International, 2009, 15, 1027-1031.	1.8	18
101	Microstructure and Mechanical Properties of Ultrafine-Grained Austenitic Oxide Dispersion Strengthened Steel. Metallurgical and Materials Transactions A: Physical Metallurgy and Materials Science, 2016, 47, 5334-5343.	1.1	18
102	Single-step plasma-induced hierarchical structures for tunable water adhesion. Scientific Reports, 2020, 10, 874.	1.6	18
103	Analysis of forging limit for sintered porous metals. Scripta Metallurgica Et Materialia, 1995, 32, 1937-1944.	1.0	17
104	Phase-field modelling of the thermo-mechanical properties of carbon steels. Acta Materialia, 2002, 50, 2259-2268.	3.8	17
105	Watching bismuth nanowires grow. Applied Physics Letters, 2011, 98, 043102.	1.5	17
106	Forming limit diagram of perforated sheet. Scripta Metallurgica Et Materialia, 1995, 33, 1201-1207.	1.0	16
107	Effect of Mn negative segregation through the thickness direction on graphitization characteristics of strip-cast white cast iron. Scripta Materialia, 2002, 46, 199-203.	2.6	16
108	Derivation of an Iron Pyrite All-Solid-State Composite Electrode with Ferrophosphorus, Sulfur, and Lithium Sulfide as Precursors. Journal of the Electrochemical Society, 2014, 161, A663-A667.	1.3	16

#	Article	IF	CITATIONS
109	Rate sensitive analysis of texture evolution in FCC metals. Metals and Materials International, 1997, 3, 252-259.	0.2	15
110	Directed assembly of fluidic networks by buckle delamination of films on patterned substrates. International Journal of Materials Research, 2007, 98, 1203-1208.	0.1	15
111	Biofunctionalized Ceramic with Self-Assembled Networks of Nanochannels. ACS Nano, 2015, 9, 4447-4457.	7.3	15
112	The influence of interfacial tensile strain on the charge transport characteristics of MoS <sub>2</sub> -based vertical heterojunction devices. Nanoscale, 2016, 8, 17598-17607.	2.8	15
113	Extremely Versatile Deformability beyond Materiality: A New Material Platform through Simple Cutting for Rugged Batteries. Advanced Engineering Materials, 2019, 21, 1900206.	1.6	15
114	Slurry-Coated Sheet-Style Sn-PAN Anodes for All-Solid-State Li-Ion Batteries. Journal of the Electrochemical Society, 2019, 166, A915-A922.	1.3	15
115	Mitigating irreversible capacity losses from carbon agents via surface modification. Journal of Power Sources, 2015, 275, 605-611.	4.0	14
116	All-solid-state disordered LiTiS2pseudocapacitor. Journal of Materials Chemistry A, 2017, 5, 15661-15668.	5.2	13
117	Structural Evolutions of Vertically Aligned Two-Dimensional MoS <sub>2</sub> Layers Revealed by in Situ Heating Transmission Electron Microscopy. Journal of Physical Chemistry C, 2019, 123, 27843-27853.	1.5	13
118	Characterization of the crystallographic microstructure of the stress-induced void in Cu interconnects. Applied Physics Letters, 2008, 92, 141917.	1.5	12
119	Evolution of a Needle Shaped Carbide in SA508 Gr3 Steel. ISIJ International, 2008, 48, 1810-1812.	0.6	12
120	Fracture Mechanics of Solder Bumps During Ball Shear Testing: Effect of Bump Size. Journal of Electronic Materials, 2009, 38, 1896-1905.	1.0	12
121	The effect of energetically coated ZrO <sub>x</sub> on enhanced electrochemical performances of Li(Ni <sub>1/3</sub> Co <sub>1/3</sub> Mn <sub>1/3</sub> )O <sub>2</sub> cathodes using modified radio frequency (RF) sputtering. Journal of Materials Chemistry A, 2015, 3, 12982-12991.	5.2	12
122	Manufacturing strategies for wafer-scale two-dimensional transition metal dichalcogenide heterolayers. Journal of Materials Research, 2020, 35, 1350-1368.	1.2	12
123	Strain Analysis of Multi-Phase Steel Using In-Situ EBSD Tensile Testing and Digital Image Correlation. Metals and Materials International, 2022, 28, 1094-1104.	1.8	12
124	Layer Orientation-Engineered Two-Dimensional Platinum Ditelluride for High-Performance Direct Alcohol Fuel Cells. ACS Energy Letters, 2021, 6, 3481-3487.	8.8	12
125	An angled nano-tunnel fabricated on poly(methyl methacrylate) by a focused ion beam. Nanotechnology, 2009, 20, 285301.	1.3	11
126	Columnar grown copper films on polyimides strained beyond 100%. Scientific Reports, 2015, 5, 13791.	1.6	11

#	Article	IF	CITATIONS
127	Self-Contained Fragmentation and Interfacial Stability in Crude Micron-Silicon Anodes. Journal of the Electrochemical Society, 2018, 165, A244-A250.	1.3	10
128	An Implantable Ionic Wireless Power Transfer System Facilitating Electrosynthesis. ACS Nano, 2020, 14, 11743-11752.	7.3	10
129	Direct recovery of spilled oil using hierarchically porous oil scoop with capillary-induced anti-oil-fouling. Journal of Hazardous Materials, 2021, 410, 124549.	6.5	10
130	Observation of the Ni <sub>2</sub> O <sub>3</sub> phase in a NiO thinâ€film resistive switching system. Physica Status Solidi - Rapid Research Letters, 2017, 11, 1700048.	1.2	9
131	Sewable soft shields for the Î <sup>3</sup> -ray radiation. Scientific Reports, 2018, 8, 1852.	1.6	9
132	Prediction of inhomogeneous texture in clad sheet metals by hot roll bond method. Metals and Materials International, 1996, 2, 133-140.	0.2	8
133	Effects of die geometry on variation of the deformation rate in equal channel angular pressing. Metals and Materials International, 2009, 15, 439-445.	1.8	8
134	1,3-Butadiene as an Adhesion Promoter Between Composite Resin and Dental Ceramic in a Dielectric Barrier Discharge Jet. Plasma Chemistry and Plasma Processing, 2013, 33, 539-551.	1.1	8
135	Dynamic recrystallization in high-purity aluminum single crystal under frictionless deformation mode at room temperature. Journal of Materials Research, 2013, 28, 2829-2834.	1.2	8
136	Contribution of the shrunk interface and the convex surface of grains on magnetic behavior in granular film. Journal of Applied Physics, 2008, 103, 07F519.	1.1	5
137	Relationship between microstructure homogeneity and bonding stability of ultrafine gold wire. Gold Bulletin, 2011, 44, 231-237.	1.1	5
138	Mechanically rollable photodetectors enabled by centimetre-scale 2D MoS2 layer/TOCN composites. Nanoscale Advances, 2021, 3, 3028-3034.	2.2	5
139	Peel-and-Stick Integration of Atomically Thin Nonlayered PtS Semiconductors for Multidimensionally Stretchable Electronic Devices. ACS Applied Materials & Interfaces, 2022, 14, 20268-20279.	4.0	5
140	Analysis of texture evolution in FCC metals by full constraint and a self-consistent viscoplastic model. Metals and Materials International, 1998, 4, 1127-1131.	0.2	4
141	The fabrication of high sensitive spin-valve sensor for magnetic bead detection. Physica Status Solidi A, 2004, 201, 1961-1964.	1.7	4
142	INVESTIGATION ON THERMAL PROPERTIES OF <font>Al</font> / <font>SiC</font> <sub><font>p</font></sub> METAL MATRIX COMPOSITE BASED ON FEM ANALYSIS. International Journal of Modern Physics B, 2008, 22, 6167-6172.	1.0	4
143	Ionâ€Beam Induced Surface Roughening of Polyâ€(methyl methacrylate) (PMMA) Tuned by a Mixture of Ar and O <sub>2</sub> Ions. Plasma Processes and Polymers, 2012, 9, 975-983.	1.6	4
144	Fabrication of wrinkled surfaces on polymer substrates by using ion implantation. Journal of the Korean Physical Society, 2012, 61, 297-300.	0.3	4

#	Article	IF	CITATIONS
145	Tensile properties of a ZnS nanowire determined with a nano-manipulator and force sensor. Journal of the Korean Physical Society, 2012, 61, 402-405.	0.3	4
146	Microstructure evolution of beryllium during proton irradiation. Journal of the Korean Physical Society, 2013, 63, 1414-1417.	0.3	4
147	Wear Behavior of Commercial Copper-Based Aircraft Brake Pads Fabricated under Different SPS Conditions. Crystals, 2021, 11, 1298.	1.0	4
148	The Thermal Annealing Effect On The Residual Stress And Interface Adhesion In The Compressive Stressed DLC Film Materials Research Society Symposia Proceedings, 2003, 795, 182.	0.1	3
149	Analysis of Alligatoring Behavior during Roll Pressing of DRI Powder with Flat Roller and Indentation-Type Roller. Materials Science Forum, 2005, 475-479, 3223-3226.	0.3	3
150	Prediction model for surface temperature of roller and densification of iron powder during hot roll pressing. International Journal of Machine Tools and Manufacture, 2007, 47, 1573-1582.	6.2	3
151	Identification of dynamic ferrite formed during the deformation of super-cooled austenite by image-based analysis of an EBSD map. Metals and Materials International, 2011, 17, 181-186.	1.8	3
152	Stability of initial texture components during deep drawing of FCC polycrystals. Metals and Materials International, 1998, 4, 489-497.	0.2	3
153	A mathematical model of unidirectional solidification in cooled mold. Metals and Materials International, 2000, 6, 189-194.	0.2	2
154	Orientation Rotation Behavior in Aluminum Alloys during Dissimilar Channel Angular Pressing. Materials Transactions, 2004, 45, 125-130.	0.4	2
155	Resistive Switching: Unraveling the Origin and Mechanism of Nanofilament Formation in Polycrystalline SrTiO <sub>3</sub> Resistive Switching Memories (Adv. Mater. 28/2019). Advanced Materials, 2019, 31, 1970205.	11.1	2
156	The cytotoxicity and skin irritation of nanostructured cellulose surface fabricated by a plasma-induced method. Cellulose, 2019, 26, 9737-9749.	2.4	2
157	Water Wetting Observation on a Superhydrophobic Hairy Plant Leaf Using Environmental Scanning Electron Microscopy. Applied Microscopy, 2016, 46, 201-205.	0.8	2
158	Analysis of texture evolution of cubic metals by isotropic and anisotropic viscoplastic self-consistent models. Metals and Materials International, 1999, 5, 17-23.	0.2	1
159	A Comparative Study of Two Shear Deforming Processes in Texture Evolution. Materials Transactions, 2005, 46, 1064-1069.	0.4	1
160	Enlargement of grain in poly-Si by adding Au in Ni-mediated crystallization of amorphous Si using a SiNx cap layer. Journal of Vacuum Science and Technology A: Vacuum, Surfaces and Films, 2005, 23, 605-608.	0.9	1
161	TENSILE PROPERTIES OF CARBON NANOFIBERS USING NANO-MANIPULATOR INSIDE SCANNING ELECTRON MICROSCOPE. International Journal of Modern Physics B, 2011, 25, 4233-4236.	1.0	1
162	Microstructural Characterization of Dehydrogenated Products of the LiBH4-YH3 Composite. Microscopy and Microanalysis, 2014, 20, 1798-1804.	0.2	1

#	Article	IF	CITATIONS
163	A Shear Strain Route Dependency of Martensite Formation in 316L Stainless Steel. Microscopy and Microanalysis, 2015, 21, 582-587.	0.2	1
164	Observation of Micro-scale Surface Morphology with Microtexture Development During Plane Strain Tensile Deformation in AZ31 Magnesium Alloy. Metallurgical and Materials Transactions A: Physical Metallurgy and Materials Science, 2015, 46, 12-17.	1.1	1
165	Exploring Lithium Deficiency in Layered Oxide Cathode for Li″on Battery. Advanced Sustainable Systems, 2017, 1, 1700026.	2.7	1
166	Multiple air-bubble enhanced oil rupture on nanostructured cellulose fabric for easy-oil cleaning fouled in a dry state. Scientific Reports, 2019, 9, 14538.	1.6	1
167	Analysis of Deformation of Porous Metals. Materials Research Society Symposia Proceedings, 1998, 521, 33.	0.1	0
168	The Stepwise Cross-sectional Crystalline Analysis of the Stress Induced Voiding in Cu Interconnect. Materials Research Society Symposia Proceedings, 2006, 914, 1.	0.1	0
169	In-situ Observation of the Formation and Growth of Twin in the Copper Electrodeposits for Ultra Large Scale Integration. Materials Research Society Symposia Proceedings, 2006, 914, 1.	0.1	0
170	3D Crystalline Structures of Stress Induced Voiding in Cu Interconnects by Focused Ion Beam and Electron Backscattered Diffraction. , 2006, , .		0
171	Contribution of Convex Surfaces to Magnetostatic Interaction in Granular Medium. IEEE Transactions on Magnetics, 2009, 45, 2655-2658.	1.2	0
172	INVESTIGATION ON THERMAL PROPERTIES OF Al/SiCp METAL MATRIX COMPOSITE BASED ON FEM ANALYSIS. , 2009, , .		0
173	Evolution of Oxide Particles during Fabrication Processes of 12Cr ODS Steel. Materials Research Society Symposia Proceedings, 2012, 1383, 41.	0.1	0
174	Formation of Ultrafine Cellular Microstructure Around Alumina Particles in a Low-Carbon Steel. Metallurgical and Materials Transactions A: Physical Metallurgy and Materials Science, 2013, 44, 4098-4105.	1.1	0
175	Experimental Measurement of Young's Modulus from a Single Crystalline Cementite. Microscopy and Microanalysis, 2014, 20, 1474-1475.	0.2	0
176	Liâ€Ion Batteries: Exploring Lithium Deficiency in Layered Oxide Cathode for Liâ€Ion Battery (Adv.) Tj ETQq0 0 0 i	gBT_/Ove	rlogk 10 Tf 5

177Grain Boundary Characteristics and Stress-induced Damage Morphologies in Sputtered and<br/>Electroplated Copper Films. Materials Research Society Symposia Proceedings, 2003, 766, 231.0.10